Journal of Neurochemistry

JOURNAL OF NEUROCHEMISTRY | 2008 | 107 | 1070–1082 doi: 10.1111/j.1471-4159.2008.05680.x

Role of methionine 35 in the intracellular Ca^{2+} homeostasis dysregulation and Ca^{2+}-dependent apoptosis induced by amyloid β-peptide in human neuroblastoma IMR32 cells

Roberto Piacentini,*,[1] Cristian Ripoli,*,[1] Lucia Leone,* Francesco Misiti,† Maria Elisabetta Clementi,‡ Marcello D'Ascenzo,* Bruno Giardina,‡ Gian Battista Azzena* and Claudio Grassi*

*Institute of Human Physiology, Medical School, Catholic University "S. Cuore", Rome, Italy

†Department of Health and Motor Sciences, University of Cassino, Cassino, Italy

‡Institute of Biochemistry and Clinical Biochemistry, Medical School, Catholic University "S. Cuore", Rome, Italy

Abstract

Amyloid β-peptide (Aβ) plays a fundamental role in the pathogenesis of Alzheimer's disease. We recently reported that the redox state of the methionine residue in position 35 of amyloid β-peptide (Aβ) 1–42 (Met35) strongly affects the peptide's ability to trigger apoptosis and is thus a major determinant of its neurotoxicity. Dysregulation of intracellular Ca^{2+} homeostasis resulting in the activation of pro-apoptotic pathways has been proposed as a mechanism underlying Aβ toxicity. Therefore, we investigated correlations between the Met35 redox state, Aβ toxicity, and altered intracellular Ca^{2+} signaling in human neuroblastoma IMR32 cells. Cells incubated for 6–24 h with 10 μM Aβ1–42 exhibited significantly increased KCl-induced Ca^{2+} transient amplitudes and resting free Ca^{2+} concentrations. Nifedipine-sensitive Ca^{2+} current densities and Ca_v1 channel expression were markedly enhanced by Aβ1–42. None of these effects were observed when cells were exposed to Aβ containing oxidized Met35 ($A\beta1–42^{Met35\text{-}Ox}$). Cell pre-treatment with the intracellular Ca^{2+} chelator 1,2-bis(2-aminophenoxy)ethane-*N,N,N′,N′*-tetraacetic acid acetoxymethyl ester (1 μM) or the Ca_v1 channel blocker nifedipine (5 μM) significantly attenuated Aβ1–42-induced apoptosis but had no effect on $A\beta1–42^{Met35\text{-}Ox}$ toxicity. Collectively, these data suggest that reduced Met35 plays a critical role in Aβ1–42 toxicity by rendering the peptide capable of disrupting intracellular Ca^{2+} homeostasis and thereby provoking apoptotic cell death.

Keywords: Alzheimer's disease, amyloid β-peptide, calcium dysregulation, Ca_v1 channels, methionine-35, neurotoxicity.

J. Neurochem. (2008) **107**, 1070–1082.

Alzheimer's disease (AD), the major cause of dementia in the elderly, is characterized by progressive cognitive decline, memory loss, and behavioral or neuropsychiatric symptoms (Selkoe 2001; Beier 2007). The neuropathological hallmarks of AD include the presence of senile plaques in the brain caused by extracellular accumulations of fibrillar amyloid β-peptides (Aβ) (Selkoe 2001). The pathophysiological significance of these peptides in AD is supported by a substantial body of evidence (Hardy and Selkoe 2002). Aβ peptides of various lengths are produced by the sequential endoproteolytic cleavage of the amyloid precursor protein by α-, β-, and γ-secretases (references in Mattson 2004). Amyloid β-peptide (Aβ) 1–40 and Aβ1–42 are the forms found most frequently in AD brains.

Numerous studies have examined the correlations between the structure and aggregation properties of Aβ peptides and their neurotoxic effects in AD (Pike *et al.* 1993; Bitan *et al.* 2003; LaFerla *et al.* 2007). The importance of the single methionine residue present in position 35

Received May 20, 2008; revised manuscript received September 1 2008; accepted September 2, 2008.

Address correspondence and reprint requests to C. Grassi, Institute of Human Physiology, Medical School, Catholic University "S. Cuore", Largo F. Vito 1, 00168 Rome, Italy. E-mail: grassi@rm.unicatt.it

[1]These authors contributed equally to this study.

Abbreviations used: AD, Alzheimer's disease; Aβ, amyloid β-peptide; BAPTA-AM, 1,2-bis(2-aminophenoxy)ethane-*N,N,N′,N′*-tetraacetic acid acetoxymethyl ester; DMSO, dimethylsulfoxide; HFIP, 1,1,1,3,3,3-Hexafluoro-2-propanol; Met35, methionine residue in position 35; MTS, 3-[(4,5-dimethylthiazol-2-yl)-5,3-carboxymethoxyphenil]-2-(4-sulfophenyl)-2H tetrazolium inner salt; PBS, phosphate buffered saline; TUNEL, Terminal Deoxynucleotide Transferase dUTP Nick End Labeling; VGCC, voltage-gated Ca^{2+} channel.

© 2008 The Authors

(Met35) of Aβ1–42 has been underscored by several groups, including our own (Ciccotosto *et al.* 2003; Butterfield and Bush 2004; Clementi *et al.* 2006; Johansson *et al.* 2007). Replacement of Met35 with either norleucine or cysteine seems to render Aβ peptides non-toxic and incapable of triggering oxidative stress responses in cells (Varadarajan *et al.* 1999; Clementi *et al.* 2006). The pivotal role played by Met35 is reflected in the inability of Aβ1–28 – which lacks this residue – to cause oxidative stress and neurotoxicity (Curtain *et al.* 2001). Indeed, several studies (including our own) have pinpointed Aβ31–35 as the shortest sequence of native peptide associated with cytotoxic effects (Iversen *et al.* 1995; Misiti *et al.* 2004, 2005; Clementi *et al.* 2005).

Amyloid β1–42 harboring the oxidized Met35 (Aβ1–$42^{Met35\text{-}Ox}$) has been found in AD brain plaques (Näslund *et al.* 1994; Kuo *et al.* 2001; Butterfield and Boyd-Kimball 2005). This residue is highly susceptible to oxidation *in vivo*, particularly under conditions of oxidative stress (Vogt 1995; Butterfield and Bush 2004; Stadtman 2004). Accumulation of Aβ1–$42^{Met35\text{-}Ox}$ in AD brains also seems to be related to reduced enzymatic reversal of methionine sulfoxide back to methionine (Prasad-Gabbita *et al.* 1999). We recently demonstrated that the neurotoxic effects of the Aβ31–35, Aβ25–35, and Aβ1–42 peptides can be significantly attenuated by oxidation of Met35 (Clementi *et al.* 2005; Misiti *et al.* 2005) whereas the presence of reduced Met35 in these peptides is associated with increases in the bax/bcl-2 ratio, which play a critical role in the pro-apoptotic effects of Aβ.

Ca^{2+} signaling is an important factor in the regulation of cell death and survival, and disruption of intracellular Ca^{2+} homeostasis has long been suspected to contribute to brain aging and to the pathogenesis of AD, both of which are characterized by impairment of the neurons' ability to control Ca^{2+} fluxes and recover from Ca^{2+} loads (Khachaturian 1984, 1989; Gibson and Peterson 1987; Landfield 1987; Disterhoft *et al.* 1994; Marx 2007; Mattson 2007; Thibault *et al.* 2007). Several comprehensive reviews have been published on mechanisms linking intracellular Ca^{2+} overloads with Aβ toxicity (LaFerla 2002; Mattson and Chan 2003; Marx 2007). Exposure of neurons to Aβ elevates intracellular Ca^{2+} levels ($[Ca^{2+}]_i$), rendering the cells vulnerable to excitotoxicity, and the neurotoxicity of Aβ has been shown to be dependent on the presence of extracellular Ca^{2+} (Mattson *et al.* 1992; Weiss *et al.* 1994; Ueda *et al.* 1997; Fu *et al.* 2006; Lopez *et al.* 2008).

These findings led us to investigate the impact of the redox state of Met35 on intracellular Ca^{2+} signals and Aβ neurotoxicity in human neuroblastoma cells. We found that intracellular Ca^{2+} homeostasis is disrupted by Aβ only when the peptide's Met35 is in the reduced state and that the attenuated toxicity of Aβ containing oxidized Met35 is correlated with the inability of this form to trigger Ca^{2+}-dependent apoptosis.

Materials and methods

Cell cultures

Human neuroblastoma IMR32 cells were cultured at 37°C in an atmosphere of 5% CO_2 in air. Cells were grown in minimum essential medium (Biochrom KG, Berlin, Germany) supplemented with 10% heat-inactivated fetal bovine serum (HyClone Lab. Inc., Logan, UT, USA), 100 IU/mL penicillin, and 100 μg/mL streptomycin (Invitrogen, Carlsbad, CA, USA). Cells were plated onto round glass coverslips (20 mm diameter) pre-coated with Growth Factor Reduced Matrigel Matrix (Becton Dickinson, Franklin Lakes, NJ, USA) and placed in 12-well plates (density, 6.0×10^4 cells/well). Neuronal differentiation of the cells was induced by adding 1 mM dibutyryl cAMP and 2.5 μM 5-bromodeoxyuridine (both from Sigma, St. Louis, MO, USA) to the culture medium. The medium was replaced the day after plating and two times a week thereafter.

Cell exposure to Aβ peptides

Amyloid β1–42 and Aβ1–42 harboring oxidized Met35 (Aβ1–$42^{Met35\text{-}Ox}$) or norleucine in the place of Met35 (Aβ1–42^{Nle35}) were purchased from Peptide Speciality Laboratories GmbH (Heidelberg, Germany). Analysis of the peptides by reverse-phase high-performance chromatography and mass spectrometry, as supplied by manufacturer, revealed a high degree of purity (> 98%). Stock solutions [1 mM in dimethylsulfoxide (DMSO)] were prepared according to the manufacturer's instructions, stored at −80°C, and thawed and diluted to the final concentration in the proper medium immediately before use. For experiments conducted to determine whether the aggregation of the peptides had any influence on the Aβ-induced effects we observed, we dissolved the Aβ1–42 peptide in 100% 1,1,1,3,3,3-Hexafluoro-2-propanol (HFIP, Sigma) (final concentration, 1 mM) to eliminate any aggregate forms that might have been present. The HFIP was then removed by vacuum evaporation, and the remaining film of disaggregated peptide was dissolved in DMSO (Aβ1–42^{HFIP}), as described above, and used immediately thereafter. In all control experiments, DMSO was added to cell cultures at the same concentrations present in the peptide solutions.

In some experiments, intracellular Ca^{2+} signaling was manipulated by exposing the cells to the selective Ca_v1 channel blocker nifedipine (5 μM), the intracellular Ca^{2+} chelator 1,2-bis(2-aminophenoxy)ethane-*N,N,N',N'*-tetraacetic acid acetoxymethyl ester (BAPTA-AM) (1 μM), the non-selective blocker of voltage-gated Ca^{2+} channels (VGCCs), Cd^{2+} (250 μM) (all from Sigma), and the $Ca_v2.2$ channel blocker ω-conotoxin GVIA (3 μM) (Alomone Labs, Gerusalem, Israel). Nifedipine-treated cultures were light-protected to prevent the drug's photodegradation.

Immunocytochemistry and TUNEL assay

IMR32 cells were processed for immunocytochemistry as previously described (D'Ascenzo *et al.* 2006; Piacentini *et al.* 2008b). Briefly, cells were fixed with 4% paraformaldehyde in phosphate buffered saline (PBS) for 10 min at 23–25°C; rinsed twice in PBS; and permeabilized with PBS/TritonX-100 (0.3%) for 15 min. Cells were then blocked with 0.3% bovine serum albumin and incubated overnight (at +4°C) with antibody against the α_{1C} subunit of $Ca_v1.2$ channels (1 : 100, Santa Cruz Biotechnology, Inc., Santa Cruz, CA, USA). The following day, cells were washed and incubated for 2 h

© 2008 The Authors
Journal Compilation © 2008 International Society for Neurochemistry,

at 23–25°C with the secondary antibody, donkey anti-goat Alexa Fluor 633 (Invitrogen), diluted 1 : 1000 in PBS. Nuclei were counter-stained for 10 min with 4′6-diamidino-2-phenylindole 2 HCl (0.5 μg/mL; Invitrogen), and the cells were coverslipped with ProLong Gold anti-fade reagent (Invitrogen) and imaged with a confocal laser scanning system (TCS-SP2, Leica Microsystems, GmbH, Wetzlar, Germany). Alexa Fluor 633 was excited with a HeNe laser, and 4′6-diamidino-2-phenylindole 2 HCl staining was imaged by 2-photon excitation (740 nm, < 140 fs, 90 MHz) performed with an ultrafast, tunable, mode-locked Ti:Saffire laser (Chameleon, Coherent Inc., Santa Clara, CA, USA).

Apoptosis was evaluated with the APO-BrdU Terminal Deoxynucleotide Transferase dUTP Nick End Labeling (TUNEL) assay kit (Invitrogen) according to the manufacturer's instructions. Briefly, cells were labeled with 5-bromo-2′-deoxyuridine-5′-triphosphate using terminal deoxynucleotide transferase. Apoptotic cells were identified immunocytochemically by means of anti-BrdU antibody labeling with Alexa Flour 488 dye, and images were obtained with the above mentioned confocal scanning system.

All experiments were repeated independently at least three times.

Cell viability

Cell survival was evaluated with the 3-[(4,5-dimethylthiazol-2-yl)-5,3-carboxymethoxyphenil]-2-(4-sulfophenyl)-2H tetrazolium inner salt (MTS) reduction assay, as previously described (Clementi *et al.* 2006). Briefly, control and Aβ-exposed cells were incubated with the MTS solution (2 mg/mL) for 4 h at 37°C in a 5% CO_2 atmosphere. Intracellular levels of soluble formazan (produced by cellular reduction of the MTS) were determined by measuring the absorbance of each 96-well plate using the automatic microplate photometer (SpectraCount, Packard Bioscience Company, Groningen, Netherlands) at a wavelength of 490 nm. The reference wavelength was 690 nm.

Reverse transcription–polymerase chain reaction

RT-PCR was performed as previously described (Clementi *et al.* 2006). Total RNA was extracted from the cells with RNA-Bee™ reagent (Biotech, Milan, Italy) used according to the supplier's instructions. RNA was quantified by optical density measurements at 260 and 280 nm with a spectrophotometer. Samples were run on a 1% agarose gel to confirm their integrity. cDNA was synthesized from 4 μg RNA in a 20-μL reaction mixture with the M-MLV Reverse Transcriptase Kit (Sigma), which was used according to the supplier's instructions. Reverse transcription products were stored at –20°C prior to use.

Polymerase chain reactions were carried out with primers synthesized by Invitrogen containing the sequences listed in the Table S1 (Chiou 2006) and Red Taq Polymerase (Sigma) used according to the supplier's instructions. Human glyceraldehyde 3-phosphate dehydrogenase (GAPDH) was used as an internal control. The reverse transcriptase reaction was carried out at 50°C for 90 min. For amplification, an initial denaturation step at 94°C for 5 min was followed by 40 cycles consisting of three temperature steps: 30 s at 94°C, 30 s at the optimal annealing PCR temperature (see Table S1), and 60 s at 72°C. Amplification was concluded with a final 10-min elongation step at 72°C.

Polymerase chain reaction products were subjected to constant-voltage electrophoresis (2 h, 80 V) on a 1.8% agarose gel with ethidium bromide (1 μg/mL) in Tris/Borate/EDTA 1× Buffer (40 mM Tris, 1 mM EDTA, 44 mM boric acid). A 123-bp ladder was used as a molecular weight marker. Images of gels were acquired (Biorad Gel Doc 2000, Hercules, CA, USA) and scanned (Biorad GS800) with Biorad Quantity One software. Results were expressed as the ratio of sample band density to the band density recorded for GAPDH.

Gel electrophoresis

The relative aggregability of the Aβ preparations used in our experiments, i.e., Aβ1–42, Aβ1–42^{HFIP}, Aβ1–$42^{Met35\text{-}Ox}$, and Aβ1–42^{Nle35}, was assessed 12 h after dilution of the peptides. Samples were diluted in NuPage sample buffer and separated by sodium dodecyl sulfate–polyacrylamide gel electrophoresis on 10–20% NuPage Tricine pre-cast gels (Invitrogen). The protein was transferred to nitrocellulose membranes (Amersham Biosciences, Buckinghamshire, UK), which were blocked for 1 h in a solution of 10% non-fat dry milk in Tris-buffered saline/Tween 20 and then incubated with 6E10 (1 : 1000) mouse monoclonal Aβ antibody (Signet, Dedham, MA, USA). For detection, the membrane was incubated with horseradish peroxidase-conjugated Ig anti-mouse antibody (1 : 2000), developed with enhanced chemiluminescence reagents (ECL, Amersham Biosciences), and exposed to Kodak X-OMAT films. Molecular mass was estimated by Rainbow Molecular Weight Markers (Amersham Biosciences) and Colorburst Electrophoresis Markers (Sigma).

Confocal Ca^{2+} imaging

Confocal Ca^{2+} imaging was performed as previously described (D'Ascenzo *et al.* 2006; Piacentini *et al.* 2008a,b). Briefly, cells were incubated for 20 min at 37°C with the Ca^{2+}-sensitive fluorescent dye Fluo-4 AM (3 μM) (Invitrogen) in Tyrode's solution containing (in mM): 150 NaCl, 4 KCl, 2 $MgCl_2$, 10 glucose, 10 (4-(2-hydroxyethil)-1-piperazineethanesulfonic acid (HEPES), and 2 $CaCl_2$. The pH was adjusted to 7.4 with NaOH. The dye-loaded cells were washed and maintained on coverslips for 20 min at 23–25°C in fresh Tyrode's solution to allow complete dye de-esterification. The coverslips were then transferred to a perfusion chamber placed on the stage of an inverted microscope (DM IRE2; Leica) attached to a confocal laser scanning system (TCS-SP2; Leica). Fluo-4-loaded cells were excited with the 488-nm line of an Ar/ArKr laser, and the emission signal was collected by a photomultiplier within a window ranging from 500 to 535 nm. Membrane depolarization was achieved by exposing the cells for 10 s to Tyrode's solution containing 50 mM KCl, and the amplitude of the intracellular Ca^{2+} transients induced by this stimulus was measured as the ΔF/F ratio, i.e., $(F_{max}\text{-}F_{pre})/(F_{pre}\text{-}F_{bgnd})$, where F_{max} represents the fluorescence recorded at the peak of KCl-induced transients calculated over all the recorded measure (60-s lasting) in a region of interest traced around each cell body; F_{pre} is the average fluorescence intensity measured during the pre-stimulus period (20 s); and F_{bgnd} is the background fluorescence measured in an area of the field lacking dye-filled structures (Takahashi *et al.* 1999). To obtain more quantitative information on basal calcium levels in control and Aβ-treated cells, intracellular Ca^{2+} concentrations were measured as previously described (Piacentini *et al.* 2008a). The following Ca^{2+} calibration formula for Fluo-4 AM was used: $[Ca^{2+}]_i = K_d*[(F_t - F_{min})/(F_{max} - F_t)]$, where F_t is the mean

© 2008 The Authors
Journal Compilation © 2008 International Society for Neurochemistry,

fluorescence intensity at *t,* the given time point; F_{max} is the fluorescence intensity recorded under calcium-saturated conditions, which were obtained by treating cells with 10 μM of the ionophore 4-bromo A-23187 (Invitrogen) dissolved in a solution containing 2 mM Ca^{2+}; F_{min} is the fluorescence intensity observed in the absence of Ca^{2+} (achieved by substituting the Ca^{2+}-containing solution with one containing 10 mM ethylene glycol-bis-(beta-aminoethylether)-*N,N,N′,N′*-tetra-acetic acid (EGTA); and K_d is the dissociation constant provided in the Fluo-4 AM datasheet (Takahashi *et al.* 1999; Cristofol *et al.* 2004; Splettstoesser *et al.* 2007). All recordings were performed at 23–25°C.

Patch-clamp recordings

Macroscopic currents flowing through VGCCs were recorded with the patch-clamp technique in the whole-cell configuration (Hamill *et al.* 1981). An Axopatch 200B amplifier (Molecular Devices, Sunnyvale, CA, USA) was used, and stimulation and data acquisition were performed with the Digidata 1200 series interface and pCLAMP 9.2 software (Molecular Devices), as previously described (Piacentini *et al.* 2008b). The external solution contained (in mM): NaCl, 125; $BaCl_2$, 10; $MgCl_2$, 1; HEPES, 10; and Tetrodotoxin, 0.1×10^{-3} to block Na^+ currents (pH adjusted to 7.3 with NaOH). The standard internal solution consisted of (in mM): CsCl, 110; tetraethyl-ammonium-Cl, 10; $MgCl_2$, 2; EGTA, 10; glucose, 8; HEPES, 10. To minimize current run-down during experiments, 4.0 mM ATP magnesium salt, 0.25 mM cAMP sodium salt, and 4.0 mM phosphocreatine disodium salt were added to this solution (pH adjusted to 7.3 with CsOH). The cell membrane was depolarized every 6 s (pulse duration, 200 ms) to voltages ranging from −40 to +40 mV from the holding potential (V_h) of −90 mV. Steady-state inactivation was studied during a test step to 0 mV following 1-s conditioning steps to potentials ranging from −80 to 0 mV. Steady-state inactivation curves were constructed in which the peak current at each potential was normalized to the maximal current. The amplitudes of 'window currents' (defined by combined plots of the activation and inactivation curves) (Antoons *et al.* 2007) were then compared in control and Aβ1–42-treated cells. Compensation for capacitative transients and leakage currents was achieved on-line with the clamp-amplifier settings and off-line by subtraction of the Cd^{2+}-insensitive (200 μM Cd^{2+}) currents. Current density (pA/pF) was calculated by dividing current amplitude by cell membrane capacitance, which was measured with the *Membrane Test* feature of the pCLAMP 9.2 software. All recordings were made at 23–25°C.

Statistics

All data are expressed as means ± SEM. Statistical analyses (Student's *t*-test and ANOVA) were performed with SYSTAT 10.2 software (Statcom, Inc., Richmond, CA, USA). The level of significance was set at 0.05.

Results

Effects of Aβ1–42 on the basal $[Ca^{2+}]_i$ and the amplitudes of spontaneous and KCl-induced Ca^{2+} transients

Membrane depolarization elicited by extracellular application of KCl (50 mM) induced clearly detectable Ca^{2+} transients in the IMR32 cells. In control cells grown for 5–6 days in differentiation medium, the mean amplitude of these transients (expressed in terms of the ΔF/F ratio) was 1.49 ± 0.03 (n = 2218). The Ca^{2+} transients were not observed when cells were depolarized in a calcium-free solution, and they were markedly reduced (−86 ± 1%; n = 244; $p < 0.001$) when the stimulus was delivered in the presence of the non-selective VGCC blocker Cd^{2+} (250 μM). These findings confirmed that the transients we recorded were dependent on Ca^{2+} influx from the extracellular medium following VGCC activation.

Additional experiments were then carried out to quantify the increases in $[Ca^{2+}]_i$ induced by KCl stimulation. At the peak of the depolarization-induced response, the mean $[Ca^{2+}]_i$ (459.1 ± 41.5 nM) was over six times higher than that recorded under basal (pre-stimulus) conditions (72.7 ± 3.1 nM) ($\Delta[Ca^{2+}]_i$ = 384.2 ± 37.5 nM, n = 216).

In cells treated for 24 h with 10 μM Aβ1–42, the mean amplitude of the KCl-induced Ca^{2+} transients was 32.2 ± 1.8% higher than that observed in controls: 2.02 ± 0.04 (n = 1553) vs. 1.49 ± 0.03 (n = 2218; $p < 0.001$; Fig. 1a). Lower Aβ1–42 concentrations (1 μM, 5 μM) produced smaller amplitude increases, and the resulting ΔF/F ratios (1.62 ± 0.08, n = 274, and 1.73 ± 0.08, n = 281, respectively) were not significantly different from those of control cells. The amplitudes of the transients also depended on the duration of cell exposure to Aβ1–42 (Fig. 1b). The maximum effects of 10 μM Aβ1–42 were observed after 12 h, when the mean ΔF/F in treated cells (n = 2471) reached 2.29 ± 0.04 (vs. 1.49 ± 0.03 in untreated controls, n = 2218, $p < 0.001$). However, the amplitudes recorded after 6, 18, and 24 h of cell exposure to Aβ1–42 were also significantly higher than those observed in control cells: ΔF/F values were 2.01 ± 0.08 (n = 537); 2.20 ± 0.12 (n = 217); and 2.02 ± 0.04 (n = 1553), respectively (F = 71.8; $p < 0.001$). In control cells exposed to the solvent alone (10 μM DMSO) for 6, 12, 18, and 24 h, no significant changes in Ca^{2+} signal amplitudes were noted at any of the time points.

In cells exposed for 24 h to 10 μM Aβ1–42, the basal $[Ca^{2+}]_i$ also rose significantly from 143.7 ± 25.3 nM (n = 268) to 692.7 ± 46.0 nM (n = 249) ($p < 0.001$).

In two control experiments we compared the effects of Aβ1–42 diluted directly in DMSO (the usual method of preparation) with those of $Aβ1–42^{HFIP}$. As shown in Fig. 2, dissolving Aβ1–42 in HFIP prior to its dilution in DMSO keeps Aβ in its monomeric form (Berman *et al.* 2008). The results obtained with these two preparations were not significantly different: after 12 h of treatment, the ΔF/F values were 1.38 ± 0.05 in control cells (n = 368); 2.33 ± 0.11 in cells exposed to Aβ1–42 dissolved in DMSO (n = 481); and 2.23 ± 0.09 in those treated with $Aβ1–42^{HFIP}$ (n = 587). Basal $[Ca^{2+}]_i$ measured after 24 h exposure to $Aβ1–42^{HFIP}$ was also not significantly different from those obtained in Aβ1–42-treated cells.

© 2008 The Authors
Journal Compilation © 2008 International Society for Neurochemistry,

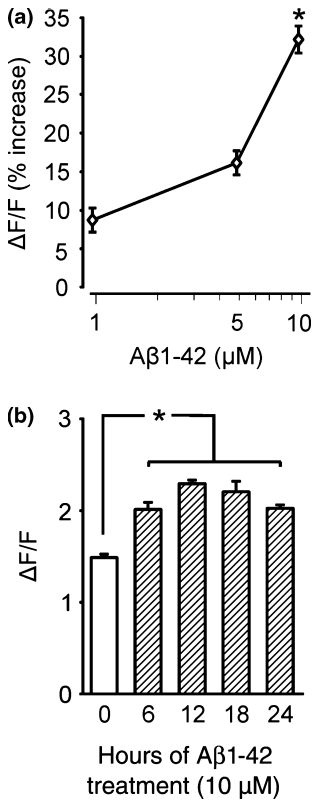

Fig. 1 Concentration- and time-dependent effects of Aβ1–42 on the amplitude of KCl-induced Ca^{2+} transients. (a) After a 24-h incubation with 10 μM Aβ1–42, signal amplitudes increased by 32.2 ± 1.8% (n = 1553) with respect to controls. Smaller, non-significant increases were also observed with lower concentrations of Aβ1–42: +8.7 ± 1.6% at 1 μM (n = 274) and +16.1 ± 1.6% at 5 μM (n = 281); (b) After 6, 12, 18, and 24 h of exposure to 10 μM Aβ1–42, the amplitudes of KCl-induced Ca^{2+} transients were significantly increased with respect to controls. Maximum effects were observed after 12 h of treatment. *p < 0.001.

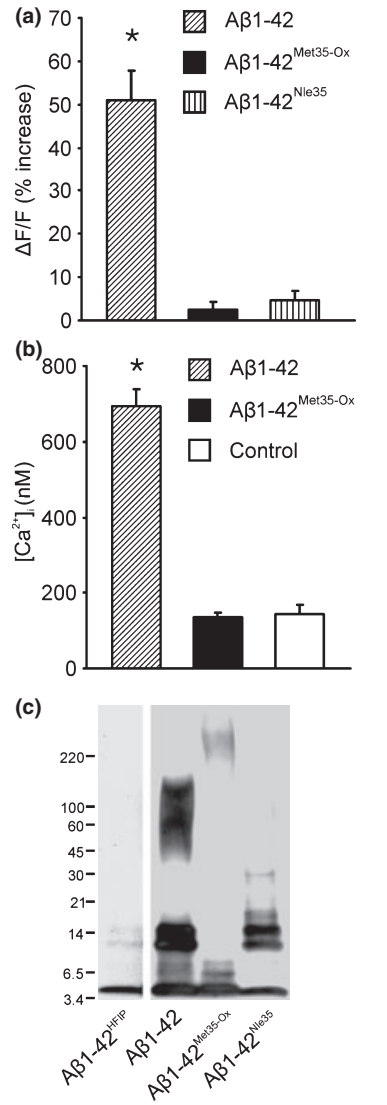

Fig. 2 Role of Met35 in the Aβ-induced increases in Ca^{2+} transient amplitudes and intracellular Ca^{2+} levels. (a) Twelve hours incubation with 10 μM Aβ1–42 significantly increased the amplitude of KCl-induced Ca^{2+} transients (+50.8 ± 6.9% with respect to controls) (*p < 0.001), but no significant changes were observed when cells were exposed for the same length of time to modified Aβ peptides in which Met35 was in the oxidized state (Aβ1–$42^{Met35-Ox}$) (mean increase, +2.5 ± 1.7%) or had been substituted with norleucine (Aβ1–42^{Nle35}) (mean increase, +4.5 ± 2.4%); (b) Incubation of IMR32 cells for 24 h with 10 μM Aβ1–$42^{Met35-Ox}$ also failed to induce the $[Ca^{2+}]_i$ increases that were observed when the unmodified Aβ1–42 peptide was used under the same conditions (mean $[Ca^{2+}]_i$ levels: 135.8 ± 11.2 nM after Aβ1–$42^{Met35-Ox}$, 692.7 ± 46.0 nM after Aβ1–42, and 143.7 ± 25.3 nM in untreated controls); (c) Western blot analysis showing the conformational species of Aβ present in the different preparations used for Ca^{2+} imaging and patch-clamp experiments.

In the absence of KCl stimulation numerous IMR32 cells exhibited spontaneous Ca^{2+} transients which varied in amplitude (ΔF/F range: 0.30–6.50) and duration (8–60 s). These Ca^{2+} signals were significantly inhibited (amplitude reduction: −66.2 ± 4.8% of controls) when Ca_v1 and $Ca_v2.2$ channels were simultaneously blocked with 5 μM nifedipine and 3 μM ω-conotoxin GVIA, which indicates that they were largely dependent on VGCC activation. After 12 h of treatment with 10 μM Aβ1–42, the amplitude and frequency of these transients increased by 50% and 60%, respectively (p < 0.001 vs. controls), significantly enhancing the overall Ca^{2+} influx.

The Aβ1–42-induced increases in Ca^{2+} transient amplitude are dependent on Met35

In previous studies we showed that the toxicity of Aβ1–42 or its fragments Aβ21–35 and Aβ25–35 in PC12 and human neuroblastoma IMR32 cells is markedly reduced by oxidation of Met35 (Misiti *et al.* 2004; Clementi *et al.* 2005, 2006). To determine whether this residue affects Aβ-

© 2008 The Authors
Journal Compilation © 2008 International Society for Neurochemistry,

mediated enhancement of KCl-induced Ca^{2+} transients, we performed Ca^{2+} imaging on cells treated with Aβ1–42 peptides in which Met35 was in the reduced state or had been oxidized to methionine sulfoxide or replaced with norleucine. As shown in Fig. 2a, after 12 h of treatment, significant increases in Ca^{2+} signal amplitudes were observed only in cells exposed to the peptide with reduced Met35. In these cells, the ΔF/F increased by 50.8 ± 6.9% ($p < 0.001$), but there were no significant changes in cells treated with Aβ1–$42^{Met35\text{-}Ox}$ (+2.5 ± 1.7%) or Aβ1–42^{Nle35} (+4.5 ± 2.4%). Reduction of Met35 thus emerged as a critical factor in the ability of Aβ to increase the amplitude of Ca^{2+} transients in our model. Cell treatment for 24 h with Aβ1–$42^{Met35\text{-}Ox}$ also failed to produce significant increases in the basal $[Ca^{2+}]_i$. The mean concentration was 135.8 ± 11.2 nM in cells treated with Aβ1–$42^{Met35\text{-}Ox}$ ($n = 104$) and 143.7 ± 25.3 nM in control cells ($n = 268$; Fig. 2b).

Aβ1–42 treatment increases macroscopic Ca^{2+} currents in IMR32 cells

The KCl-induced Ca^{2+} transients whose amplitude is modulated by Aβ1–42 treatment are caused by VGCC activation, as demonstrated by their marked inhibition in the presence of Cd^{2+}. To further investigate the effects of Aβ treatment on Ca^{2+} influx through these channels, we measured Ba^{2+} currents in whole-cell patch-clamp experiments. In cells exposed for 12 h to 10 μM Aβ1–42, peak Ba^{2+} currents were significantly larger than those recorded in controls (−248.8 ± 19.5 vs. −110.9 ± 10.7 pA; $n = 34$ for each group; $p < 0.001$), but exposure to Aβ1–$42^{Met35\text{-}Ox}$ had no significant effect (mean Ba^{2+} current amplitude, −136.8 ± 14.4 pA; $n = 19$). Membrane capacitance was not significantly affected by either treatment (10.3 ± 0.3, 10.0 ± 0.3, and 9.6 ± 0.4 pF in control, Aβ1–42-treated, and Aβ1–$42^{Met35\text{-}Ox}$-treated cells, respectively). Therefore, Ba^{2+} current density was significantly increased (+121%) by Aβ1–42 only when the peptide's Met35 was in the reduced state (24.9 ± 1.9 vs. 11.3 ± 1.2 pA/pF in untreated controls; $p < 0.001$): treatment with Aβ1–$42^{Met35\text{-}Ox}$ had no significant effect on the current density (13.9 ± 1.2 pA/pF; $n = 19$; Fig. 3).

Cell treatment with Aβ1–42, but not with Aβ1–$42^{Met35\text{-}Ox}$, increases Ca_v1 channel expression and function

Human neuroblastoma IMR32 cells express several types of high voltage-activated Ca^{2+} channels, and their relative densities vary during cell differentiation (Carbone *et al.* 1990; Grassi *et al.* 1994). The results of this study and previous research by our group (Grassi *et al.* 1994, 2004; D'Ascenzo *et al.* 2002) show that the $Ca_v2.2$ and Ca_v1 channels account respectively for 70–80% and 10–25% of the total high voltage-activated currents in these cells. To determine whether Aβ selectively targets one of these two Ca^{2+} channel subtypes, we recorded Ba^{2+} currents in Aβ-treated and control cells before and after the application of

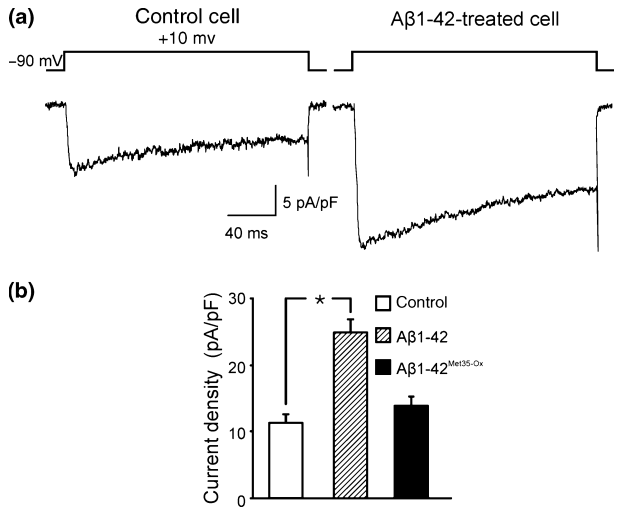

Fig. 3 Aβ1–42 increases macroscopic Ba^{2+} currents in IMR32 cells. (a) Representative traces of macroscopic Ba^{2+} current density in controls and Aβ1–42-treated cells (10 μM for 12 h); (b) After 12 h of cell treatment with 10 μM Aβ1–42, mean current density was significantly higher (+121%) than that observed in controls (24.9 ± 1.9 vs. 11.3 ± 1.2 pA/pF, respectively), but cell treatment with 10 μM Aβ1–$42^{Met35\text{-}Ox}$ had no significant effect (13.9 ± 1.2 pA/pF). *$p < 0.001$.

5 μM nifedipine, which selectively and reversibly blocks Ca_v1 channels. As shown in Fig. 4, the peak Ca_v1 current density (estimated by subtracting the post-nifedipine current traces recorded at 0 mV from those recorded before nifedipine application) was 2.9 ± 0.3 pA/pF ($n = 33$) in control cells. It was markedly increased after 12 h of treatment with 10 μM Aβ1–42 (10.9 ± 0.9 pA/pF; $n = 30$; $p < 0.001$) but virtually unaffected by cell exposure to Aβ1–$42^{Met35\text{-}Ox}$ (3.0 ± 0.3 pA/pF, $n = 19$). Significant increases in Ca_v1 current densities were induced by Aβ1–42 treatment at all potentials ranging from −10 to +30 mV (Fig. 4b), but there were no changes in the activation curve, steady-state inactivation and 'window currents', expressed as the area under the activation and the inactivation curves (Antoons *et al.* 2007). Aβ1–42 treatment also increased the density of the nifedipine-insensitive (non-Ca_v1) currents (15.4 ± 1.4 vs. 8.5 ± 1.0 pA/pF in controls; $n = 30$; $p < 0.005$) although this increase (+81%) was much smaller than that observed in the Ca_v1 currents (+276%).

These findings were especially interesting in light of the specific role played by Ca^{2+} signaling through Ca_v1 channels in the regulation of cell survival and death. We decided therefore to investigate the effects of Aβ1–42 on the expression of the pore-forming α_{1C} subunit of the heteromeric $Ca_v1.2$ channels (Fig. 4d–f). In immunocytochemical assays, control cells exhibited very weak α_{1C} labeling, which was not significantly modified by Aβ1–$42^{Met35\text{-}Ox}$ treatment. In contrast, the Aβ1–42-exposed cells exhibited much more intense, diffuse Ca_v1-channel immunolabeling. These findings suggest that the presence of Met35 in the reduced state

© 2008 The Authors
Journal Compilation © 2008 International Society for Neurochemistry,

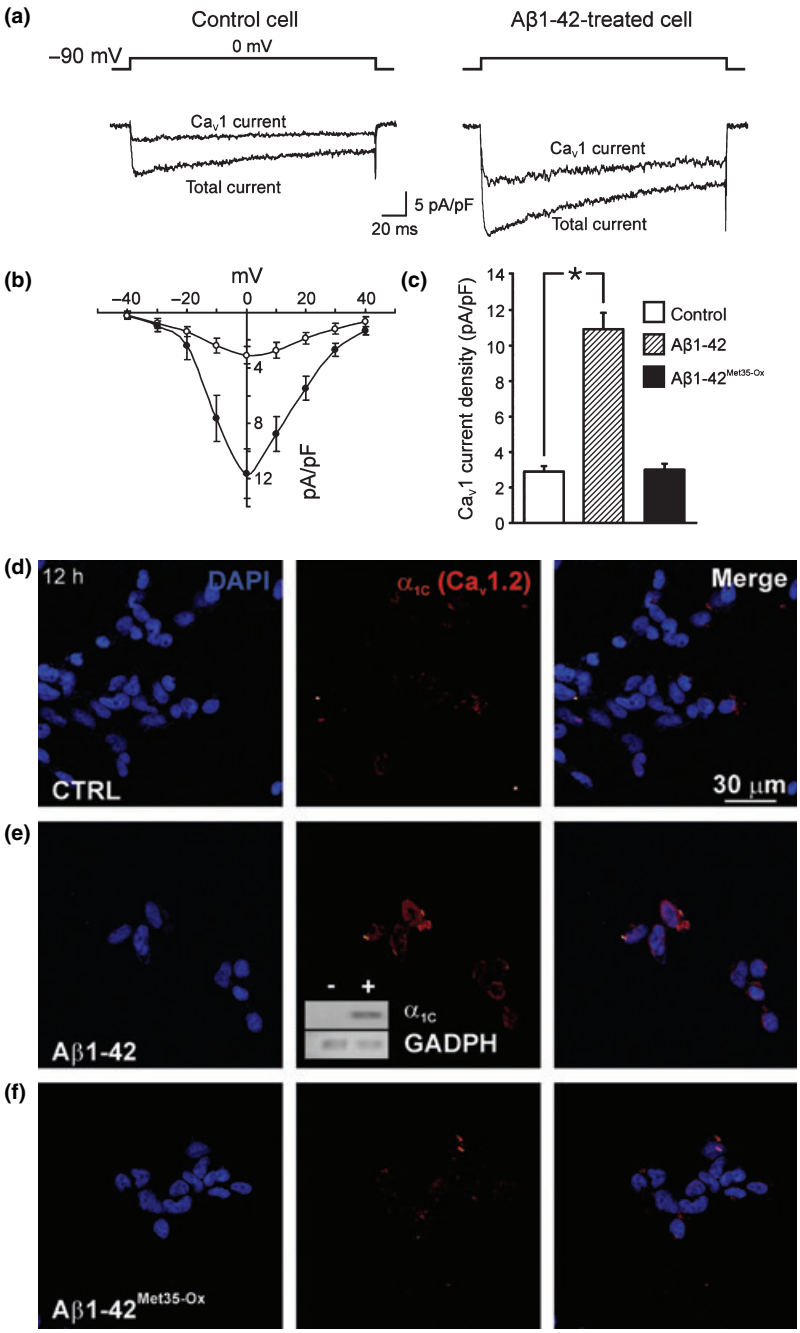

Fig. 4 Aβ-induced effects on Ca_v1 channel expression and function are dependent on the redox state of Met35. (a) Representative traces of total and nifedipine-sensitive Ba^{2+} current density in control and Aβ1–42-treated cells (10 μM for 12 h); (b) Current-to-voltage curves in control (O) and Aβ1–42-treated cells (●) were obtained by averaging data from 15 cells; (c) Mean Ca_v1 current density significantly increased from 2.9 ± 0.3 to 10.9 ± 0.9 pA/pF (+276%; $^*p < 0.001$) after 12 h of cell treatment with 10 μM Aβ1–42, but no significant changes were observed when cells were treated for the same interval with Aβ1–$42^{Met35\text{-}Ox}$ (3.0 ± 0.3 pA/pF); (d–f) Immunocytochemistry revealed markedly increased expression of the α_{1C} subunit of Ca_v1 channels in cultures treated for 12 h with 10 μM Aβ1–42, but not in those exposed for the same period of time to Aβ1–$42^{Met35\text{-}Ox}$. Insert of panel (e) shows increased α_{1C} subunit mRNA expression revealed by RT-PCR: the band density ratio α_{1C}/glyceraldehyde 3-phosphate dehydrogenase (GAPDH) was 2.51 in Aβ1–42-treated cells versus 0.03 of controls.

is essential to Aβ's ability to up-regulate Ca_v1 channel expression, and this conclusion is further supported by the results of RT-PCR experiments, which revealed increased α_{1C} mRNA expression in cells treated with 10 μM Aβ1–42 (Fig. 4e, inset).

Role of Met35 in the Ca^{2+}-dependent apoptosis induced by Aβ

Our next step was to investigate the possible correlations among the reduced state of Met35, intracellular Ca^{2+} overload, and neuronal apoptosis. Analyses of DNA fragmentation in IMR32 cells with the TUNEL assay (Fig. 5a–d) revealed similarly low rates of apoptosis (< 10%) in control cultures and those exposed for 24 h to 10 μM Aβ1–42^{Nle35} (Fig. 5e). However, the percentage of $TUNEL^+$ cells tripled (28.5 ± 2.0%) after treatment with 10 μM of Aβ1–$42^{Met35\text{-}Ox}$, and it was more than five times higher than controls (50.5 ± 5.1%) in cultures exposed to Aβ1–42 (Fig. 5e). Similar results emerged when cell viability was measured with the MTS assay. Viable cell rates were significantly

© 2008 The Authors
Journal Compilation © 2008 International Society for Neurochemistry,

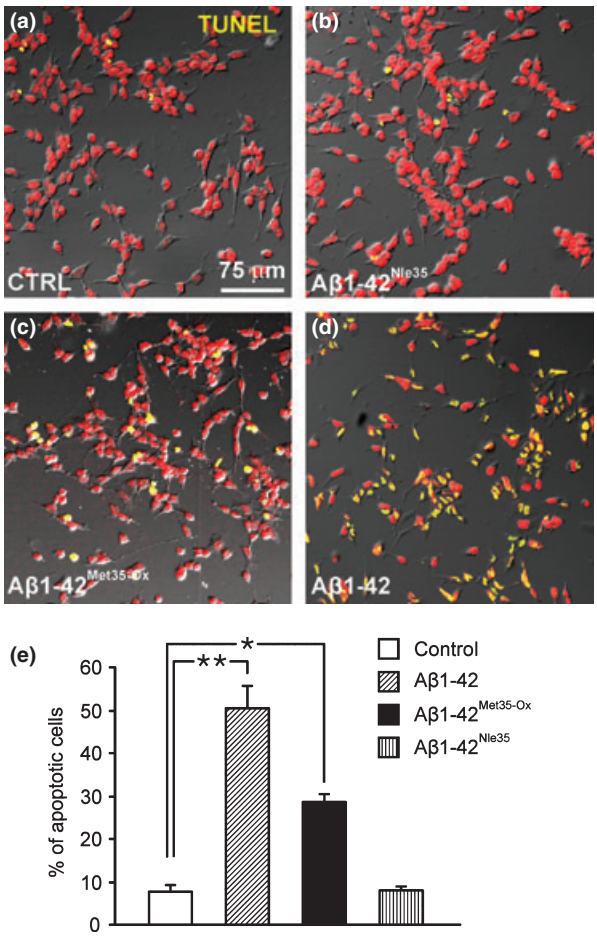

Fig. 5 Aβ-induced apoptosis is dependent on the redox state of Met35. Representative examples of TUNEL labeling of IMR32 cells (40× microscopic fields): (a) TUNEL positivity was limited to a few cells (7.7 ± 1.5%) in control cultures, and (b) no significant changes were observed in cultures treated for 24 h with 10 μM Aβ1–42^{Nle35} (8.0 ± 0.9% of total cells); (c) When IMR32 cells were exposed to 10 μM Aβ1–$42^{Met35\text{-}Ox}$ for 24 h, TUNEL labeling rates rose to 28.5 ± 2.0%, and (d) 24 h of treatment with Aβ1–42 produced even more markedly increases (50.5 ± 5.1%); (e) Bar gram showing the mean values for each condition (each based on rates observed in 10 fields) *$p < 0.01$; **$p < 0.001$.

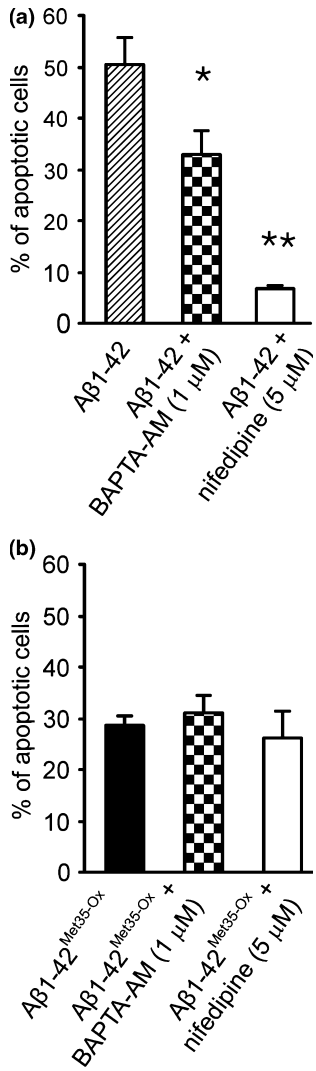

Fig. 6 Intracellular Ca^{2+} buffering and Ca_v1 channel blockade counteract Aβ1–42-induced toxicity but have no influence on the effects produced by Aβ1–$42^{Met35\text{-}Ox}$. (a) In IMR32 cells cultured with the intracellular Ca^{2+} chelator BAPTA-AM (1 μM), exposure to Aβ1–42 was associated with significantly lower rates of apoptosis (mean TUNEL-positivity rate, 32.8 ± 4.8%) than those observed when Aβ1–42 was applied in the absence of Ca^{2+} buffering (50.5 ± 5.1%). The protective effects of the selective Ca_v1 channel blocker nifedipine (5 μM) were even more evident (mean TUNEL-positivity rate, 6.9 ± 0.6%); (b) Neither BAPTA-AM nor nifedipine had any significant effect on apoptotic cell rates produced by exposure to 10 μM Aβ1–$42^{Met35\text{-}Ox}$ (TUNEL-positivity rates: 28.5 ± 2.0% in the absence of Ca^{2+} modulation, 31.2 ± 3.3% and 26.2 ± 5.3% in cultures pre-treated with BAPTA-AM and nifedipine, respectively). *$p < 0.05$; **$p < 0.001$.

decreased by 24 h of cell treatment with Aβ1–42 or Aβ1–$42^{Met35\text{-}Ox}$ (62.0 ± 7.1% and 82.0 ± 7.1% of controls, respectively; $p < 0.001$), but they were unaffected by exposure to Aβ1–42^{Nle35} (95.0 ± 5.0%).

To determine whether these effects were dependent on the intracellular Ca^{2+} overload produced by Aβ, we repeated TUNEL and MTS assays in cells cultured with either the intracellular Ca^{2+} chelator BAPTA-AM or the Ca_v1 channel antagonist nifedipine. As shown in Fig. 6a, cell pre-treatment with 1 μM BAPTA-AM significantly inhibited the pro-apoptotic action of Aβ1–42: the mean percentage of total cells displaying TUNEL positivity decreased from 50.5 ± 5.1 to 32.8 ± 4.8% ($p < 0.05$). Treatment with nifedipine (5 μM) produced even stronger protective effects: TUNEL-positivity rates dropped to 6.9 ± 0.6% ($p < 0.001$), a value comparable to that observed in control cultures. When cell viability was assessed with the MTS assay, a

© 2008 The Authors

similar picture emerged: inhibition of intracellular Ca^{2+} signals with calcium chelation or Ca_v1 channel blockade significantly increased the percentage of viable cells observed after Aβ1–42 treatment [88.5 ± 4.9% in Aβ1–42 + BAPTA-AM-treated cells ($p < 0.05$) and 92.5 ± 2.0% ($p < 0.001$) in Aβ1–42 + nifedipine-treated cells, compared with 62.0 ± 7.1% in cultures treated with Aβ1–42 alone]. In contrast, the mild toxic effects of $Aβ1–42^{Met35\text{-}Ox}$ (apoptotic cell rate, 28.5 ± 2.0%) were not significantly influenced by BAPTA-AM (31.2 ± 3.3%) or nifedipine (26.2 ± 5.3%) in TUNEL experiments (Fig. 6b) or MTS assays (cell viability rates: 83.0 ± 7.1% in cultures pre-treated with BAPTA-AM, 84.5 ± 5.0% in those pre-treated with nifedipine, and 82.0 ± 7.1% in those subjected to no manipulation of intracellular Ca^{2+}).

These findings suggest that the Met35-dependent toxicity of Aβ1–42 in IMR32 neuroblastoma cells is correlated with apoptosis triggered by the disruption of intracellular Ca^{2+} homeostasis.

Discussion

A substantial body of research indicates that accumulation of amyloid β-peptide in the brain plays a causal role in AD, but some of the molecular mechanisms underlying this action have yet to be defined (for reviews see LaFerla 2002; LaFerla *et al.* 2007; Mattson 2007). Aβ1–40 and Aβ1–42, the forms most frequently found in human AD brains, have different biochemical properties, and the 42-residue peptide also displays significantly greater neurotoxicity (Davis and Van Nostrand 1996; Klein *et al.* 1999; Dahlgren *et al.* 2002; Saido and Iwata 2006; Yun *et al.* 2007). Several studies indicate that the peptide's Met35 residue plays a key role in Aβ toxicity (Varadarajan *et al.* 1999; Ciccotosto *et al.* 2003; Butterfield and Bush 2004; Clementi *et al.* 2006; Johansson *et al.* 2007). The sulfur atom in this residue may be in either the oxidized or reduced state, and Aβ peptides containing both forms of Met35 have been isolated in variable amounts from plaques found post-mortem in AD patients' brains (Näslund *et al.* 1994; Kuo *et al.* 2001; Butterfield and Bush 2004).

We provide novel evidence that the redox status of Met35 is a critical determinant of Aβ1–42 toxicity, which influences the peptide's ability to disrupt intracellular Ca^{2+} homeostasis, thereby triggering apoptotic cell death. We have already demonstrated that replacement of Met35 with norleucine (which is structurally similar to methionine but lacks the latter's sulfur atom) virtually annuls Aβ1–42's toxicity, and markedly diminished toxicity is observed when the Met35 residue is oxidized (Clementi *et al.* 2006).

The involvement of calcium in the pathogenesis of AD was first proposed in 1989 by Khachaturian (see LaFerla 2002 for review). Since then numerous studies have documented associations between the neurotoxic effects of cerebral Aβ deposition and loss of intracellular Ca^{2+} homeostasis resulting from modulation of the influx of Ca^{2+} from the extracellular space and its release from intracellular stores (Davidson *et al.* 1994; Ueda *et al.* 1997; MacManus *et al.* 2000; He *et al.* 2002; LaFerla 2002; Mattson and Chan 2003; Smith *et al.* 2005; Lopez *et al.* 2008). Various mechanisms have been proposed to explain how Aβ perturbs the intracellular Ca^{2+} environment, including the formation of calcium-conducting pores in lipid bilayers (Arispe *et al.* 1993) and modulation of the activity of Ca^{2+} permeable ion channels, e.g., NMDA receptors, nicotinic receptors, and VGCCs (Ueda *et al.* 1997; Dougherty *et al.* 2003; Mattson 2007; Lopez *et al.* 2008). With reference to the VGCCs, several groups have reported that Aβ increases the expression and activation of Ca_v1 channels (Davidson *et al.* 1994; Ueda *et al.* 1997; Ekinci *et al.* 1999; MacManus *et al.* 2000; Scragg *et al.* 2005; Smith *et al.* 2005; Fu *et al.* 2006; Lopez *et al.* 2008), and these effects have been attributed to various mechanisms, including free radical activity (Ueda *et al.* 1997), mitogen-activated protein kinase phosphorylation, and increased traffiking of channels to plasma membrane (Scragg *et al.* 2005).

However, key questions regarding Aβ-induced neurotoxicity and the precise role of Ca^{2+} in the pathogenesis of AD remain unanswered. And no information is available on the role played by the redox state of Met35 in Aβ-induced dysregulation of Ca^{2+} homeostasis. These issues were specifically addressed in the present study. Our Ca^{2+} imaging experiments revealed that Aβ-mediated derangement of the Ca^{2+} regulatory machinery is specifically dependent on the redox state of Met35. Unlike $Aβ1–42^{Met35\text{-}Ox}$ and $Aβ1–42^{Nle35}$, Aβ1–42 produced dose- and time-dependent increases in the amplitude of spontaneous and depolarization-induced Ca^{2+} transients with maximum effects (increases of approximately 50% for both parameters) observed after 12 h of exposure to Aβ1–42. These effects markedly increased basal intracellular Ca^{2+} concentrations (approximately +400% after 24 h treatment with Aβ1–42) whereas cell exposure to $Aβ1–42^{Met35\text{-}Ox}$ had no effect whatsoever on the $[Ca^{2+}]_i$. In addition, whole-cell patch-clamp recordings showed that Aβ significantly enhances Ba^{2+} current densities when its Met35 is reduced but not when this residue is oxidized to methionine sulfoxide or replaced with norleucine. Marked increases (+276%) in Ca_v1 current densities were also observed only with Aβ1–42. Our PCR and immunofluorescence experiments confirmed that exposing cells to this peptide significantly up-regulates the expression of the α_{1C} subunit of Ca_v1 channels (at both the mRNA and protein levels), but no effects of this type were seen in cells treated with $Aβ1–42^{Met35\text{-}Ox}$.

The many functions attributed to Ca^{2+} signaling in neurons include the regulation of cell survival (Orrenius *et al.* 2003; Toescu *et al.* 2004; Mattson 2007) and the inability of certain

© 2008 The Authors
Journal Compilation © 2008 International Society for Neurochemistry,

neurons to maintain Ca^{2+} homeostasis is widely recognized as an important co-factor in the pathogenesis of AD (LaFerla 2002; Mattson 2004; Green and LaFerla 2008; Lopez *et al.* 2008). We recently demonstrated that treatment of hippocampal neurons with trimethyltin, a neurotoxic compound used to generate *in vivo* and *in vitro* models of AD, causes cytoplasmic accumulation of Ca^{2+} that triggers apoptosis (Piacentini *et al.* 2008b).

In the present study we attempted to determine whether the differential toxicity exhibited by Aβ1–42 and Aβ1–$42^{Met35\text{-}Ox}$ in IMR32 cells (Clementi *et al.* 2006) is because of former peptide's ability to up-regulate Ca_v1 channel expression and activity. The results support our hypothesis that the redox state of Met35 is a pivotal factor in the ability of Aβ to activate Ca^{2+}-dependent pro-apoptotic pathways. In TUNEL assays, Aβ1–42 emerged as a much more potent inducer of DNA-fragmentation in neuroblastoma cells than Aβ1–$42^{Met35\text{-}Ox}$, and this difference correlated with the differential effects of the two peptides on caspase-3 activation and on the bax/bcl-2 ratio (Clementi *et al.* 2006). The greater neurotoxicity of Aβ1–42 is clearly dependent on the dysregulation of Ca^{2+} homeostasis it produces. In fact, Aβ1–42-induced apoptosis was strongly attenuated by calcium buffering with BAPTA-AM and even more markedly inhibited by nifedipine's antagonism of Ca_v1 channels, but neither of these Ca^{2+}-modulating agents had any significant effect on the mildly pro-apoptotic action of Aβ1–$42^{Met35\text{-}Ox}$. The mechanisms underlying Aβ-induced apoptosis thus appear to differ depending on the redox state of Met35: the effects of peptides containing reduced Met35 seem to be Ca^{2+}-dependent while Aβ harboring oxidized Met35 apparently acts in a Ca^{2+}-independent manner. Our demonstration of the Ca^{2+}-independent neurotoxicity produced by Aβ1–$42^{Met35\text{-}Ox}$ might also help to explain why only modest clinical improvement has been observed in AD patients treated with the Ca_v1 channel antagonist nimodipine (López-Arrieta and Birks 2002). The striking efficacy of nifedipine in protecting IMR32 cells from Aβ1–42 toxicity is consistent with the well documented specific involvement of Ca_v1 channel activity in the regulation of cell survival and death (Nicotera and Orrenius 1998; Tao *et al.* 1998; Berridge *et al.* 2000; Dolmetsch *et al.* 2001; West *et al.* 2001; Toescu *et al.* 2004; Webster *et al.* 2006; Li *et al.* 2007). The protection afforded by intracellular Ca^{2+} buffering is less specific. It is also important to recall that the buffering effects produced by the BAPTA concentrations used in our experiments simply lowered $[Ca^{2+}]_i$. Complete buffering would, *per se*, cause cell death.

Taken together, the results of the present study suggest that, in our experimental model, the differential toxicity of Aβ peptides containing oxidized or reduced Met35 depends on the ability of the latter form to activate Ca^{2+}-dependent pro-apoptotic pathways by enhancing Ca_v1 channel expression and function. This does not exclude the possibility that other mechanisms also contribute to this difference. Oxidation of Met35 has been reported to cause conformational changes in Aβ1–42, which delay the formation of oligomers, protofibrils, and fibrils (Hou *et al.* 2002; Butterfield and Bush 2004; Johansson *et al.* 2007). Correlation between the capacity for aggregation and the neurotoxic potentials of Aβ peptides has been demonstrated in numerous studies (Johansson *et al.* 2007; LaFerla *et al.* 2007; Walsh and Selkoe 2007). Nonetheless, the impact of the Met35 redox status on Aβ neurotoxicity observed in our study seems to be largely independent of Aβ aggregation. The results of our experiments seem to suggest that there is no correlation between the capacities for aggregation of the different Aβ peptides we used and their influence on intracellular calcium signaling. In fact, the effects produced by Aβ dissolved in HFIP prior to its dilution in DMSO (a step shown to break up small Aβ aggregates that have formed) were virtually identical to those achieved without HFIP pre-treatment. And, solutions of Aβ1–42^{Nle35}, which were characterized by Aβ oligomer levels similar to those found in Aβ1–42 directly diluted in DMSO, had no effects whatsoever on the regulation of intracellular Ca^{2+} levels.

In conclusion, we provide novel evidence of the impact of the Met35 redox status on the neurotoxicity exhibited by Aβ. The presence of a reduced Met35 allows the peptide to up-regulate Ca_v1 channel expression and enhance intracellular Ca^{2+} signaling, effects that lead to the activation of Ca^{2+}-dependent pro-apoptotic pathways. This Ca^{2+}-mediated toxicity can be effectively counteracted by selective pharmacological blockade of Ca_v1 channel activity and to a lesser extent by intracellular Ca^{2+} chelation. In contrast, the admittedly milder but by no means negligible toxicity produced by Aβ peptides containing oxidized Met35 seems to be based on Ca^{2+}-independent mechanisms, and for this reason it is likely to be refractory to therapeutic interventions aimed at restoring intracellular Ca^{2+} homeostasis.

Acknowledgements

This work was supported by grants from the Italian Ministry of Education University and Research (PRIN2007), ISS, and the Catholic University (D1 funds) to C.G.. We wish to thank Mr. Daniele Mezzogori for technical assistance.

Supporting information

Additional Supporting Information may be found in the online version of this article:

Table S1. The sequences of the primers and the predicted sizes of PCR products.

Please note: Wiley-Blackwell are not responsible for the content or functionality of any supporting materials supplied by the authors. Any queries (other than missing material) should be directed to the corresponding author for the article.

© 2008 The Authors
Journal Compilation © 2008 International Society for Neurochemistry,

References

Antoons G., Volders P. G. A., Stankovicova T., Bito V., Stengl M., Vos M. A. and Sipido K. R. (2007) Window Ca^{2+} current and its modulation by Ca^{2+} release in hypertrophied cardiac myocytes from dogs with chronic atrioventricular block. *J. Physiol.* **579.1**, 147–160.

Arispe N., Rojas E. and Pollard H. B. (1993) Alzheimer disease amyloid beta protein forms calcium channels in bilayer membranes: blockade by tromethamine and aluminum. *Proc. Natl Acad. Sci. USA* **90**, 567–571.

Beier M. T. (2007) Treatment strategies for the behavioral symptoms of Alzheimer's disease: focus on early pharmacologic intervention. *Pharmacotherapy* **27**, 399–411.

Berman D. E., Dall'armi C., Voronov S. V., McIntire L. B., Zhang H., Moore A. Z., Staniszewski A., Arancio O., Kim T. W. and Di Paolo G. (2008) Oligomeric amyloid-beta peptide disrupts phosphatidylinositol-4,5-bisphosphate metabolism. *Nat. Neurosci.* **11**, 547–554.

Berridge M. J., Lipp P. and Bootman M. D. (2000) The versatility and universality of calcium signalling. *Nat. Rev. Mol. Cell. Biol.* **1**, 11–21.

Bitan G., Kirkitadze M. D., Lomakin A., Vollers S. S., Benedek G. B. and Teplow D. B. (2003) Amyloid beta-protein (Abeta) assembly: Abeta 40 and Abeta 42 oligomerize through distinct pathways. *Proc. Natl Acad. Sci. USA* **100**, 330–335.

Butterfield D. A. and Boyd-Kimball D. (2005) The critical role of methionine 35 in Alzheimer's amyloid beta-peptide (1–42)-induced oxidative stress and neurotoxicity. *Biochim. Biophys. Acta* **1703**, 149–156.

Butterfield D. A. and Bush A. I. (2004) Alzheimer's amyloid beta-peptide (1–42): involvement of methionine residue 35 in the oxidative stress and neurotoxicity properties of this peptide. *Neurobiol. Aging* **25**, 563–568.

Carbone E., Sher E. and Clementi F. (1990) Ca^{2+} currents in human neuroblastoma IMR32 cells: kinetics, permeability and pharmacology. *Pflügers Arch.* **416**, 170–179.

Chiou W. F. (2006) Effect of Abeta exposure on the mRNA expression patterns of voltage-sensitive calcium channel alpha 1 subunits (alpha 1A-alpha 1D) in human SK-N-SH neuroblastoma. *Neurochem. Int.* **49**, 256–261.

Ciccotosto G. D., Barnham K., Cherny R. A., Masters C. L., Bush A. I., Curtain C. C., Cappai R. and Tew D. (2003) Methionine oxidation: implication for the mechanism of toxicity of the amyloid peptide from Alzheimer's disease. *Lett. Pept. Sci.* **10**, 413–417.

Clementi M. E., Marini S., Coletta M., Orsini F., Giardina B. and Misiti F. (2005) Abeta(31-35) and Abeta(25-35) fragments of amyloid beta-protein induce cellular death through apoptotic signals: role of the redox state of methionine-35. *FEBS Lett.* **579**, 2913–2918.

Clementi M. E., Pezzotti M., Orsini F., Sampaolese B., Mezzogori D., Grassi C., Giardina B. and Misiti F. (2006) Alzheimer's amyloid beta-peptide (1–42) induces cell death in human neuroblastoma via bax/bcl-2 ratio increase: an intriguing role for methionine 35. *Biochem. Biophys. Res. Commun.* **342**, 206–213.

Cristofol R. M., Gasso S., Vilchez D., Pertusa M., Rodriguez-Farre E. and Sanfeliu C. (2004) Neurotoxic effects of trimethyltin and triethyltin on human fetal neuron and astrocyte cultures: a comparative study with rat neuronal cultures and human cell lines. *Toxicol. Lett.* **152**, 35–46.

Curtain C. C., Ali F., Volitakis I., Cherny R. A., Norton R. S., Beyreuther K., Barrow C. J., Masters C. L., Bush A. I. and Barnham K. J. (2001) Alzheimer's disease amyloid-beta binds copper and zinc to generate an allosterically ordered membrane-penetrating structure containing superoxide dismutase-like subunits. *J. Biol. Chem.* **276**, 20466–20473.

D'Ascenzo M., Martinotti G., Azzena G. B. and Grassi C. (2002) cGMP/protein kinase G-dependent inhibition of N-type Ca^{2+} channels induced by nitric oxide in human neuroblastoma IMR32 cells. *J. Neurosci.* **22**, 7485–7492.

D'Ascenzo M., Piacentini R., Casalbore P., Budoni M., Pallini R., Azzena G. B. and Grassi C. (2006) Role of L-type Ca^{2+} channels in neural stem/progenitor cell differentiation. *Eur. J. Neurosci.* **23**, 935–944.

Dahlgren K. N., Manelli A. M., Stine Jr W. B., Baker L. K., Krafft G. A. and LaDu M. J. (2002) Oligomeric and fibrillar species of amyloid-beta peptides differentially affect neuronal viability. *J. Biol. Chem.* **277**, 32046–32053.

Davidson R. M., Shajenko L. and Donta T. S. (1994) Amyloid beta-peptide (Abeta P) potentiates a nimodipine-sensitive L-type barium conductance in N1E-115 neuroblastoma cells. *Brain Res.* **643**, 324–327.

Davis J. and Van Nostrand W. E. (1996) Enhanced pathologic properties of Dutch-type mutant amyloid beta-protein. *Proc. Natl Acad. Sci. USA* **93**, 2996–3000.

Disterhoft J. F., Moyer Jr J. R. and Thompson L. T. (1994) The calcium rationale in aging and Alzheimer's disease. Evidence from an animal model of normal aging. *Ann. N Y Acad. Sci.* **747**, 382–406.

Dolmetsch R. E., Pajvani U., Fife K., Spotts J. M. and Greenberg M. E. (2001) Signaling to the nucleus by an L-type calcium channel-calmodulin complex through the MAP kinase pathway. *Science* **294**, 333–339.

Dougherty J. J., Wu J. and Nichols R. A. (2003) Beta-amyloid regulation of presynaptic nicotinic receptors in rat hippocampus and neocortex. *J. Neurosci.* **23**, 6740–6747.

Ekinci F. J., Malik K. U. and Shea T. B. (1999) Activation of the L voltage-sensitive calcium channel by mitogen-activated protein (MAP) kinase following exposure of neuronal cells to beta-amyloid. MAP kinase mediates beta-amyloid-induced neurodegeneration. *J. Biol. Chem.* **274**, 30322–30327.

Fu H., Li W., Lao Y. *et al.* (2006) Bis(7)-tacrine attenuates beta amyloid-induced neuronal apoptosis by regulating L-type calcium channels. *J. Neurochem.* **98**, 1400–1410.

Gibson G. E. and Peterson C. (1987) Calcium and the aging nervous system. *Neurobiol. Aging* **8**, 329–343.

Grassi C., Magnelli V., Carabelli V., Sher E. and Carbone E. (1994) Inhibition of low- and high-threshold Ca^{2+} channels of human neuroblastoma IMR32 cells by Lambert-Eaton myasthenic syndrome (LEMS) IgGs. *Neurosci. Lett.* **181**, 50–56.

Grassi C., D'Ascenzo M., Torsello A., Martinotti G., Wolf F., Cittadini A. and Azzena G. B. (2004) Effects of 50 Hz electromagnetic fields on voltage-gated Ca^{2+} channels and their role in modulation of neuroendocrine cell proliferation and death. *Cell Calcium* **35**, 307–315.

Green K. M. and LaFerla F. M. (2008) Linking Ca^{2+} to Aβ and Alzheimer's Disease. *Neuron* **59**, 190–194.

Hamill O. P., Marty A., Neher E., Sakmann B. and Sigworth F. J. (1981) Improved patch-clamp techniques for high-resolution current recording from cells and cell-free membrane patches. *Pflügers Arch.* **391**, 85–100.

Hardy J. and Selkoe D. J. (2002) The amyloid hypothesis of Alzheimer's disease: progress and problems on the road to therapeutics. *Science* **297**, 353–356.

He L. M., Chen L. Y., Lou X. L., Qu A. L., Zhou Z. and Xu T. (2002) Evaluation of beta-amyloid peptide 25–35 on calcium homeostasis in cultured rat dorsal root ganglion neurons. *Brain Res.* **939**, 65–75.

Hou L., Kang I., Marchant R. E. and Zagorski M. G. (2002) Methionine 35 oxidation reduces fibril assembly of the amyloid abeta-(1–42) peptide of Alzheimer's disease. *J. Biol. Chem.* **277**, 40173–40176.

© 2008 The Authors
Journal Compilation © 2008 International Society for Neurochemistry,

Iversen L. L., Mortishire-Smith R. J., Pollack S. J. and Shearman M. S. (1995) The toxicity in vitro of beta-amyloid protein. *Biochem. J.* **311**, 1–16.

Johansson A. S., Bergquist J., Volbracht C., Päiviö A., Leist M., Lannfelt L. and Westlind-Danielsson A. (2007) Attenuated amyloid-beta aggregation and neurotoxicity owing to methionine oxidation. *Neuroreport* **18**, 559–563.

Khachaturian Z. S. (1984) Scientific challenges and opportunities related to Alzheimer's disease. *Clin. Pharm.* **3**, 522–523.

Khachaturian Z. S. (1989) The role of calcium regulation in brain aging: reexamination of a hypothesis. *Aging* **1**, 17–34.

Klein A. M., Kowall N. W. and Ferrante R. J. (1999) Neurotoxicity and oxidative damage of beta amyloid 1–42 versus beta amyloid 1-40 in the mouse cerebral cortex. *Ann. N Y Acad. Sci.* **893**, 314–320.

Kuo Y. M., Kokjohn T. A., Beach T. G. *et al.* (2001) Comparative analysis of amyloid-beta chemical structure and amyloid plaque morphology of transgenic mouse and Alzheimer's disease brains. *J. Biol. Chem.* **276**, 12991–12998.

LaFerla F. M. (2002) Calcium dyshomeostasis and intracellular signalling in Alzheimer's disease. *Nat. Rev. Neurosci.* **3**, 862–872.

LaFerla F. M., Green K. N. and Oddo S. (2007) Intracellular amyloid-beta in Alzheimer's disease. *Nat. Rev. Neurosci.* **8**, 499–509.

Landfield P. W. (1987) 'Increased calcium-current' hypothesis of brain aging. *Neurobiol. Aging* **8**, 346–347.

Li X. M., Yang J. M., Hu D. H. *et al.* (2007) Contribution of downregulation of L-type calcium currents to delayed neuronal death in rat hippocampus after global cerebral ischemia and reperfusion. *J. Neurosci.* **27**, 5249–5259.

Lopez J. R., Lyckman A., Oddo S., Laferla F. M., Querfurth H. W. and Shtifman A. (2008) Increased intraneuronal resting [Ca^{2+}] in adult Alzheimer's disease mice. *J. Neurochem.* **105**, 262–271.

López-Arrieta J. M. and Birks J. (2002) Nimodipine for primary degenerative, mixed and vascular dementia. *Cochrane Database Syst. Rev.* **1**, CD000147.

MacManus A., Ramsden M., Murray M., Henderson Z., Pearson H. A. and Campbell V. A. (2000) Enhancement of 45Ca^{2+} influx and voltage-dependent Ca^{2+} channel activity by beta-amyloid-(1-40) in rat cortical synaptosomes and cultured cortical neurons. Modulation by the proinflammatory cytokine interleukin-1beta. *J. Biol. Chem.* **275**, 4713–4718.

Marx J. (2007) Alzheimer's disease. Fresh evidence points to an old suspect: calcium. *Science* **318**, 384–385.

Mattson M. P. (2004) Pathways towards and away from Alzheimer's disease. *Nature* **430**, 631–639.

Mattson M. P. (2007) Calcium and neurodegeneration. *Aging Cell* **6**, 337–350.

Mattson M. P. and Chan S. L. (2003) Neuronal and glial calcium signaling in Alzheimer's disease. *Cell Calcium* **34**, 385–397.

Mattson M. P., Cheng B., Davis D., Bryant K., Lieberburg I. and Rydel R. E. (1992) beta-Amyloid peptides destabilize calcium homeostasis and render human cortical neurons vulnerable to excitotoxicity. *J. Neurosci.* **12**, 376–389.

Misiti F., Martorana G. E., Nocca G., Di Stasio E., Giardina B. and Clementi M. E. (2004) Methionine 35 oxidation reduces toxic and pro-apoptotic effects of the amyloid beta-protein fragment (31-35) on isolated brain mitochondria. *Neuroscience* **126**, 297–303.

Misiti F., Sampaolese B., Pezzotti M., Marini S., Coletta M., Ceccarelli L., Giardina B. and Clementi M. E. (2005) Abeta(31-35) peptide induce apoptosis in PC 12 cells: contrast with Abeta(25-35) peptide and examination of underlying mechanisms. *Neurochem. Int.* **46**, 575–583.

Näslund J., Schierhorn A., Hellman U. *et al.* (1994) Relative abundance of Alzheimer Aβ amyloid peptide variants in Alzheimer disease and normal aging. *Proc. Natl Acad. Sci. USA* **91**, 8378–8382.

Nicotera P. and Orrenius S. (1998) The role of calcium in apoptosis. *Cell Calcium* **23**, 173–180.

Orrenius S., Zhivotovsky B. and Nicotera P. (2003) Regulation of cell death: the calcium-apoptosis link. *Nat. Rev. Mol. Cell. Biol.* **4**, 552–565.

Piacentini R., Gangitano C., Ceccariglia S., Fà A. D., Azzena G. B., Michetti F. and Grassi C. (2008a) Dysregulation of intracellular calcium homeostasis is responsible for neuronal death in an experimental model of selective hippocampal degeneration induced by trimethyltin. *J. Neurochem.* **105**, 2109–2121.

Piacentini R., Ripoli C., Mezzogori D., Azzena G. B. and Grassi C. (2008b) Extremely low-frequency electromagnetic fields promote in vitro neurogenesis via upregulation of Ca_V1-channel activity. *J. Cell. Physiol.* **215**, 129–139.

Pike C. J., Burdick D., Walencewicz A. J., Glabe C. G. and Cotman C. W. (1993) Neurodegeneration induced by beta-amyloid peptides in vitro: the role of peptide assembly state. *J. Neurosci.* **13**, 1676–1687.

Prasad-Gabbita S., Aksenov M. Y., Lovell M. A. and Markesbery W. R. (1999) Decrease in peptide methionine sulfoxide reductase in Alzheimer's disease brain. *J. Neurochem.* **73**, 1660–1666.

Saido T. C. and Iwata N. (2006) Metabolism of amyloid beta peptide and pathogenesis of Alzheimer's disease. Towards presymptomatic diagnosis, prevention and therapy. *Neurosci. Res.* **54**, 235–253.

Scragg J. L., Fearon I. M., Boyle J. P., Ball S. G., Varadi G. and Peers C. (2005) Alzheimer's amyloid peptides mediate hypoxic up-regulation of L-type Ca^{2+} channels. *FASEB J.* **19**, 150–152.

Selkoe D. J. (2001) Alzheimer's disease: genes, proteins, and therapy. *Physiol. Rev.* **81**, 741–766.

Smith I. F., Green K. N. and LaFerla F. M. (2005) Calcium dysregulation in Alzheimer's disease: recent advances gained from genetically modified animals. *Cell Calcium* **38**, 427–437.

Splettstoesser F., Florea A. M. and Büsselberg D. (2007) IP3 receptor antagonist, 2-APB, attenuates cisplatin induced Ca^{2+}-influx in HeLa-S3 cells and prevents activation of calpain and induction of apoptosis. *Br. J. Pharmacol.* **151**, 1176–1186.

Stadtman E. R. (2004) Cyclic oxidation and reduction of methionine residues of proteins in antioxidant defense and cellular regulation. *Arch. Biochem. Biophys.* **423**, 2–5.

Takahashi A., Camacho P., Lechleiter J. D. and Herman B. (1999) Measurement of intracellular calcium. *Physiol. Rev.* **79**, 1089–1125.

Tao X., Finkbeiner S., Arnold D. B., Shaywitz A. J. and Greenberg M. E. (1998) Ca^{2+} influx regulates BDNF transcription by a CREB family transcription factor-dependent mechanism. *Neuron* **20**, 709–726.

Thibault O., Gant J. C. and Landfield P. W. (2007) Expansion of the calcium hypothesis of brain aging and Alzheimer's disease: minding the store. *Aging Cell* **6**, 307–317.

Toescu E. C., Verkhratsky A. and Landfield P. W. (2004) Ca^{2+} regulation and gene expression in normal brain aging. *Trends Neurosci.* **27**, 614–620.

Ueda K., Shinohara S., Yagami T., Asakura K. and Kawasaki K. (1997) Amyloid beta protein potentiates Ca^{2+} influx through L-type voltage-sensitive Ca^{2+} channels: a possible involvement of free radicals. *J. Neurochem.* **68**, 265–271.

Varadarajan S., Yatin S., Kanski J., Jahanshahi F. and Butterfield D. A. (1999) Methionine residue 35 is important in amyloid beta-peptide-associated free radical oxidative stress. *Brain Res. Bull.* **50**, 133–141.

Vogt W. (1995) Oxidation of methionyl residues in proteins: tools, targets, and reversal. *Free Radic. Biol. Med.* **18**, 93–105.

© 2008 The Authors
Journal Compilation © 2008 International Society for Neurochemistry,

Walsh D. M. and Selkoe D. J. (2007) A beta oligomers – a decade of discovery. *J. Neurochem.* **101**, 1172–1184.

Webster N. J., Ramsden M., Boyle J. P., Pearson H. A. and Peers C. (2006) Amyloid peptides mediate hypoxic increase of L-type Ca^{2+} channels in central neurones. *Neurobiol. Aging* **27**, 439–445.

Weiss J. H., Pike C. J. and Cotman C. W. (1994) Ca^{2+} channel blockers attenuate beta-amyloid peptide toxicity to cortical neurons in culture. *J. Neurochem.* **62**, 372–375.

West A. E., Chen W. G., Dalva M. B., Dolmetsch R. E., Kornhauser J. M., Shaywitz A. J., Takasu M. A., Tao X. and Greenberg M. E. (2001) Calcium regulation of neuronal gene expression. *Proc. Natl Acad. Sci. USA* **98**, 11024–11031.

Yun S., Urbanc B., Cruz L., Bitan G., Teplow D. B. and Stanley H. E. (2007) Role of electrostatic interactions in amyloid beta-protein (A beta) oligomer formation: a discrete molecular dynamics study. *Biophys. J.* **92**, 4064–4077.

© 2008 The Authors
Journal Compilation © 2008 International Society for Neurochemistry,